Detailed investigation of self-imaging in large-core multimode optical fibers for application in fiber lasers and amplifiers

X. Zhu, A. Schülzgen, H. Li, L. Li, L. Han, J. V. Moloney, and N. Peyghambarian

College of Optical Sciences, University of Arizona, 1641 East University Boulevard, Tucson, Arizona 85721, USA
xszhu@email.arizona.edu

Abstract: Properties of the self-imaging effect based on multimode interference (MMI) in large-core passive optical fibers are investigated and analyzed in detail, with the purpose of using multimode active fibers for high power single-transverse-mode emission. Although perfect self-imaging of the input field from a standard single-mode fiber (SMF-28) in a multimode fiber becomes practically impossible as its core diameter is larger than 50 μm, a quasi-reproduction of the input field occurs when the phase difference between the excited modes and the peak mode inside the multimode fiber is very small. Our simulation and experimental results indicate that, if the length of the multimode fiber segment can be controlled accurately, reproduction of the input field with a self-imaging quality factor larger than 0.9 can be obtained. In this case, a low-loss hybrid fiber cavity composed of a SMF-28 segment and a very-large-core active multimode fiber segment can be built. It is also found that for the hybrid fiber cavity, increasing the mode-field diameter of the single-mode fiber improves both the self-imaging quality and the tolerance on the required length accuracy of the multimode fiber segment. Moreover, in this paper key parameters for the design of MMI-based fiber devices are defined and their corresponding values are provided for multimode fibers with core diameters of 50 μm and 105 μm.

OCIS codes: (060.2320) Fiber optics amplifiers and oscillators; (140.3510) Fiber lasers; (140.4780) Optical oscillators; (060.2270) Fiber characterization.

References and links

1. H. F. Talbot, "Facts relating to optical science No. IV," Phil Mag. **9**, 15-22 (1836).
2. O. Bryngdahl, "Image formation using self-imaging techniques," J. Opt. Soc. Am. **63**, 416-419 (1973).
3. R. Ulrich and G. Ankele, "Self-imaging in homogeneous planar optical waveguides," Appl. Phys. Lett. **27**, 337-339 (1975).
4. L. B. Soldano and E. C. M. Penning, "Optical multi-mode interference devices based on self-imaging: principles and applications," J. Lightwave Technol. **13**, 615-627, (1995).
5. S. W. Allison and G. T. Gillies, "Observations of and applications for self-imaging in optical fibers," Appl. Opt. **33**, 1802-1805 (1994).
6. R. Selvas, I. Torres-Gomez, A. Martinez-Rios, J. A. Alvarez-Chavez, D. A. May-Arrioja, P. Likamwa, A. Mehta, and E. G.. Johnson, "Wavelength tuning of fiber lasers using multimode interference effects," Opt. Express **13**, 9439-9445, (2005).
7. W. S. Mohammed, P. W. E. Smith, and X. Gu, "All-fiber multimode interference bandpass filter," Opt. Lett. **31**, 2547-2549, (2006).
8. W. S. Mohammed, A. Mehta, and E. G. Johnson, "Wavelength tunable fiber lens based on multimode interference," J. Lightwave Technol. **22**, 469-477, (2004).
9. A. Mehta, W. S. Mohammed, and E. G. Johnson, "Multimode interference-based fiber-optic displacement sensor," IEEE Photon. Technol. Lett. **15**, 1129-1131, (2003).
10. K. Hamamoto, E. Gini, C. Holtmann, and H. Melchior, "Single-transverse-mode active multi-mode-interferometer 1.45 μm high power laser diode," Appl. Phys. B **73**, 571-574 (2001).
11. H. J. Baker, J. R. Lee, and D. R. Hall, "Self-imaging and high-beam-quality operation in multi-mode planar waveguide optical amplifiers," Opt. Express **10**, 297-302 (2002).

#100268 - $15.00 USD Received 18 Aug 2008; revised 18 Sep 2008; accepted 28 Sep 2008; published 2 Oct 2008

12. W. S. Pelouch, D. D. Smith, J. E. Koroshetz, I. T. Mckinnie, J. R. Unternahrer, S. W. Henderson, W. R. Scharpf, "Self-imaging in waveguide lasers and amplifiers", OSA Topical Meeting on Advanced Solid State Lasers, 6-9 (Optical Society of America, Washington, D. C., 2002).
13. I. T. Mckinnie, J. E. Koroshetz, W. S. Pelouch, D. D. Smith, J. R. Unternahrer, S. W. Henderson, M. Wright, "Self-imaging waveguide Nd:YAG laser with 58% slope efficiency," OSA Topical Meeting on Advanced Solid State Lasers, 262-263 (Optical Society of America, Washington, D. C., 2002).
14. I. T. Mckinnie, B. E. Callicoatt, C. Wood, J. E. Koroshetz, J. R. Unternahrer, M. L. Tartaglia, S. E. Christensen, O. J. Koski, M. Hinckley, M. J. Bellanca, E. Schneider, and D. D. Smith, "Self-imaging waveguide lasers," Conference on Lasers and Electro-optics, **CMS1**, 319-321 (2005).
15. V. Raghunathan, H. Renner, R. R. Rice, and B. Jalali, "Self-imaging silicon Raman amplifier," Opt. Express **15**, 3396-3408 (2007).
16. X. Zhu, A. Schülzgen, H. Li, L. Li, Q. Wang, S. Suzuki, V. L. Temyanko, J. V. Moloney, and N. Peyghambarian, "Single-transverse-mode output from a fiber laser based on multimode interference," Opt. Lett. **33**, 908-910 (2008).
17. H. Li, M. Brio, L. Li, A. Schülzgen, N. Peyghambarian, and J. V. Moloney, "Multimode interference in circular step-index fibers studies with the mode expansion approach," J. Opt. Soc. Am. B **24**, 2707-2720 (2007).
18. J. Limpert, N. D. Robin, I. M. Honninger, F. Salin, F. Roser, A. Liem, T. Schreiber, S. Nolte, H. Zellmer, A. Tunnermann, J. Broeng, A. Petersson, C. Jakobsen, "High-power rod-type photonic crystal fiber laser," Opt. Express **13**, 1055-1058 (2005).

1. Introduction

The phenomenon that a spatially periodic electromagnetic field can reproduce itself periodically along the propagation direction as a result of diffraction, called the self-imaging effect, was observed for the first time by Talbot [1] in 1836. Self-imaging in uniform index slab waveguides, suggested by Bryngdahl [2], was first demonstrated by Ulrich [3] and was found to be an inherent property of multimode (MM) waveguides. In homogenous MM waveguides, the self-imaging effect can be understood as a consequence of constructive multimode interference (MMI). As an arbitrary electromagnetic field is coupled into a MM waveguide, a specific set of eigenmodes of the MM waveguide is excited and each of them propagates along the waveguide independently with its own propagation constant. Although the superposition of these excited modes generally yields a complicated field distribution due to multiple interferences, self-imaging of the input field can be obtained at certain positions where the excited modes are in phase.

After the first demonstration of MMI-based self-imaging in planar waveguide, MMI in planar waveguides has been intensively investigated and the self-imaging effect has been widely utilized in the design and fabrication of high-performance waveguide couplers [4]. Although MMI in cylindrical optical fibers is more complicated than that in planar waveguides, the self-imaging effect in MM fibers was first observed by Allison [5] and has been experimentally demonstrated by several groups in recent years for various applications such as wavelength tunable laser [6], all-fiber bandpass filter [7], wavelength tunable fiber lens [8], and fiber-optic displacement sensor [9].

In addition to many applications of MMI-based self-imaging in passive waveguides, utilizing self-imaging in active MM waveguides is attracting more and more interest. Applying self-imaging to obtain single-transverse-mode emission from an active MM planar waveguide has been proposed and demonstrated as a route to overcome the constraints of an active single-mode (SM) waveguide [10-15]. A MMI-based fiber laser generating SM emission from an active MM fiber has also been recently demonstrated [16]. In contrast to other approaches of obtaining SM emission from active MM fibers, this MMI fiber laser provided a perfect beam quality ($M^2 = 1.01$), an efficiency close to that of the corresponding MM fiber laser, and an inherent narrow bandwidth. Although the first MMI fiber laser has shown some remarkable properties, the core diameter of the active MM fiber was only 25 μm making it comparable to core sizes of active SM fibers with low numerical aperture (NA). To take full advantage of this new approach for SM fiber lasers and amplifiers, MMI has to be investigated for large-core (> 50 μm) MM fibers.

When the core diameter of the MM fiber segment is 25 μm [16], MMI in the fiber is relatively simple and an almost perfect reproduction of the input SM field from a SMF-28

#100268 - $15.00 USD Received 18 Aug 2008; revised 18 Sep 2008; accepted 28 Sep 2008; published 2 Oct 2008

fiber can be obtained because only three modes are strongly excited in the MM segment. As the core diameter increases, more modes are excited and MMI becomes rather complicated. Fully understanding the characteristics of self-imaging in large-core MM fibers is necessary and instructive for further design of MMI fiber lasers and amplifiers with large-core active fibers. Moreover, compared to the intensive and thorough investigations of self-imaging in planar waveguides, there are few physical insights into self-imaging in MM fibers, even though a lot of fiber devices based on MMI have been demonstrated. Therefore, a detailed investigation of the self-imaging properties of MM fibers is also beneficial for the design and optimization of the MMI fiber devices that have been demonstrated previously [6-9]. In this paper, the principle of self-imaging in MM fibers is briefly reiterated first. Then the properties of self-imaging in MM fibers are investigated in detail through theoretical calculations and experiments of self-imaging in passive MM fibers with a NA of 0.22 and core diameters of 50 μm and 105 μm, respectively. The fully vectorial mode expansion approach, developed by Li [17], is used to do the calculations.

2. Principle of self-imaging in multimode fibers

Since the mathematical description of MMI-based self-imaging in MM fibers is available in the literature [4], the principle of self-imaging is summarized rather briefly.

To investigate the self-imaging properties of MM fibers, a simple MMI structure is employed, where a SM fiber segment is directly spliced to a MM fiber segment, as depicted in Fig. 1.

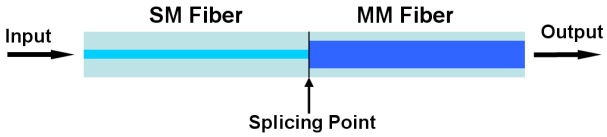

Fig. 1. A simple fiber structure for studying the self-imaging properties of MM optical fibers.

In the plane of the splicing point (z = 0), the propagating field inside the SM fiber can be decomposed into the guided modes of the MM fiber [4], i.e.,

$$E_{SM}(r,\phi,z=0)=\sum_{1}^{N}C_n e_n(r,\phi,z=0), \tag{1}$$

where $E_{SM}(r,\phi,z=0)$ is the fundamental mode of the SM fiber and $e_n(r,\phi,z=0)$ is the *n*-th guided mode of the MM fiber. N is the number of excited modes inside the MM fiber. C_n is the mode expansion coefficient and can be determined from [7]

$$C_n=\frac{\iint_S E_{SM}(r,\phi)\times e_n^*(r,\phi)ds}{\iint_S \left|e_n(r,\phi)\right|^2 ds}. \tag{2}$$

Neglecting mode conversion, all excited modes propagate independently inside the MM fiber, and the field $E_{MM}(r,\phi,z)$ along the MM fiber can be expressed as

$$E_{MM}(r,\phi,z)=\sum_{1}^{N}C_n e_n(r,\phi,0)e^{-i\beta_n z}=e^{-i\beta_1 z}\sum_{1}^{N}C_n e_n(r,\phi,0)e^{-i(\beta_n-\beta_1)z}, \tag{3}$$

#100268 - $15.00 USD Received 18 Aug 2008; revised 18 Sep 2008; accepted 28 Sep 2008; published 2 Oct 2008

where β_1 and β_n are the propagation constants of the fundamental mode and the *n*-th excited mode of the MM fiber, respectively.

Clearly, at certain positions inside the MM fiber, the reproduction of the input field occurs, i.e., $E_{MM}(r,\phi,z_{self-imaging}) = E_{SM}(r,\phi,z=0)$, if the following condition is satisfied for all N modes

$$(\beta_n - \beta_1) z_{self-imaging} = \Delta\beta_n z_{self-imaging} = m_n 2\pi . \qquad (m_n \text{ integer}) \qquad (4)$$

Eq. (4) implies that the phase different between any two excited modes is an integer multiple of 2π, i.e., all excited modes are in phase.

For MM fibers with core diameters of 50 μm and 105 μm and a numerical aperture of 0.22, only the first seven and fourteen HE modes are found to be strongly excited, respectively, due to the mode orthogonality and the on-axis excitation. The field distributions of the excited modes and their in-phase supposition are illustrated in Figs. 2(a) and 2(b), respectively. Clearly, if all the excited modes are in phase, a precise self-imaging of the input field occurs.

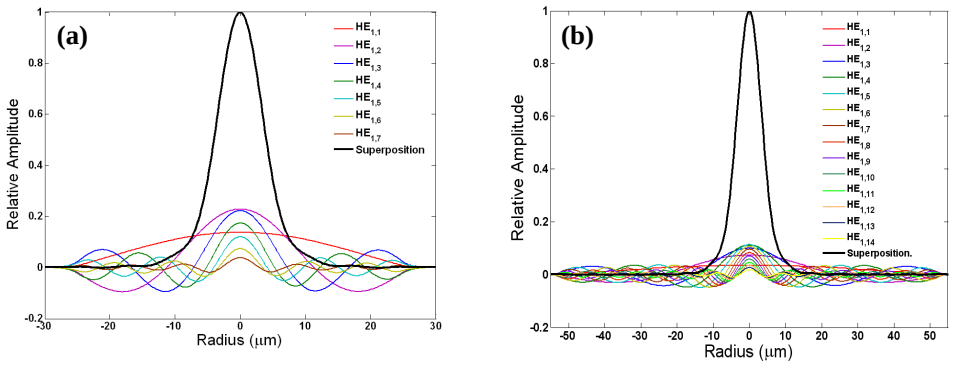

Fig. 2. Field distributions of the excited modes and their in-phase superposition in the MM fiber segment of the MMI structure. (a) Core diameter of the MM fiber is 50 μm; (b) Core diameter of the MM fiber is 105 μm.

3. Properties of self-imaging in large-core multimode optical fibers

3.1 Self-imaging quality

As shown in Fig. 2, the input field can be reproduced through superposition and in-phase interference of the excited modes. However, because seven or fourteen HE modes are excited in the 50 μm or 105 μm MM fibers, respectively, and their propagation constants do not show any multiple relationships between each other, all the phase differences between the excited modes cannot be made simultaneously integer multiples of 2π. Consequently, the reproductions show aberrations and the self-imaging quality factor, also defined as an effective amplitude reflection coefficient γ in [17] by Eq. (27), will be less than 1. The quality factor γ of self-imaging of a single-frequency (λ = 1.535 μm) input field from a standard SM fiber (SMF-28) are plotted in Figs. 3(a) and 3(b) for the MM fibers with core diameters of 50 μm and 105 μm, respectively. In both cases, perfect self-imaging (γ = 1) cannot be obtained. However, a quasi-reproduction of the input field with a large self-imaging quality factor (for instance, γ > 0.9) still occurs at certain positions inside the MM fiber. For example, a self-image of the input field with γ > 0.97 can be obtained at z = 10.3 mm in the 50 μm or 43.28 mm in the 105 μm MM fiber, respectively. In both cases, the energy percentage of the excited

#100268 - $15.00 USD Received 18 Aug 2008; revised 18 Sep 2008; accepted 28 Sep 2008; published 2 Oct 2008

modes and the phase differences between all the other excited modes and the peak mode (the most strongly excited mode) are plotted in Figs. 4(a) and 4(b), respectively. Clearly, self-imaging, strictly speaking, the quasi-reproduction of the input field, occurs even when the phase differences between the excited modes are slightly different from 2π. E.g., in the case of a 105 μm MM fiber [see Fig. 4(b)] almost perfect self-imaging with $\gamma > 0.97$ is achieved despite phase mismatches up to 0.02π for strongly excited modes and up to 0.15π for modes with smaller contributions.

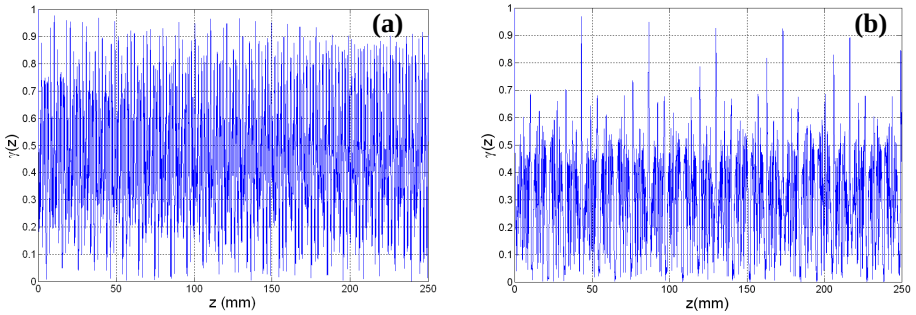

Fig. 3. Self-imaging quality factor γ along the MM fiber segment with a core diameter of (a) 50 μm or (b) 105 μm, respectively.

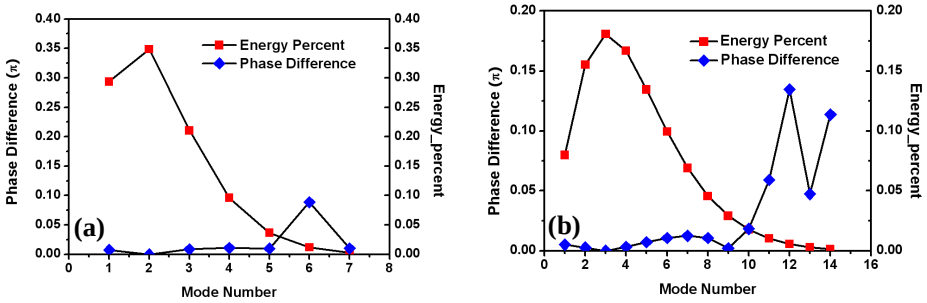

Fig. 4. Energy percentage of the excited modes and the phase differences at a self-imaging point between the excited modes and the mode of highest intensity inside MM fiber with core diameters of (a) 50 μm and (b) 105 μm fiber, respectively.

It is straightforward that the self-imaging quality should reduce with the core diameter of the MM fiber segment. To see how the self-imaging quality changes with the core diameter, the maximum quality factor γ within a 1 m MM fiber segment with respect to the core diameter is plotted in Fig. 5(a). As the core diameter of the MM fiber segment is larger than 250 μm, the self-imaging quality reduces evidently with the core diameter. When the core diameter is 500 μm, the self-imaging quality factor is only 0.69.

3.2 Self-imaging length interval

In Fig. 3, the self-imaging length interval inside the 50 μm fiber is about 10.3 mm and that inside the 105 μm fiber is about 43.28 mm. It is obvious that, as the core size increases, the self-imaging length interval or the self-imaging period increases accordingly, as a result of more excited modes. The variation of the self-imaging length interval with the core size of a

#100268 - $15.00 USD Received 18 Aug 2008; revised 18 Sep 2008; accepted 28 Sep 2008; published 2 Oct 2008

MM fiber is plotted in Fig. 5(b). Since self-imaging is never 100% perfect, periodical peaks whose γ values are clearly larger than those of neighboring maxima are defined as the self-imaging peaks. It is found that the self-imaging length interval $L_{self\text{-}imaging}$ increases quadratically with the core diameter d_m and $L_{self\text{-}imaging} = 4040 d_m^2/mm$ is a very good approximation. For instance, when the core diameter is 200 μm, $L_{self\text{-}imaging}$ = 153.8 mm. It means that the length of the MM fiber segment must be multiple of 153.8 mm to obtain high quality self-imaging. As analyzed below, short-length (tens of centimeters) active MM fibers are preferred for MMI fiber lasers and amplifiers because mode conversion, a major factor for MMI cavity loss, increases with the fiber core size and the fiber length. Therefore, when a large-core MM fiber is used, its length should be chosen with more considerations.

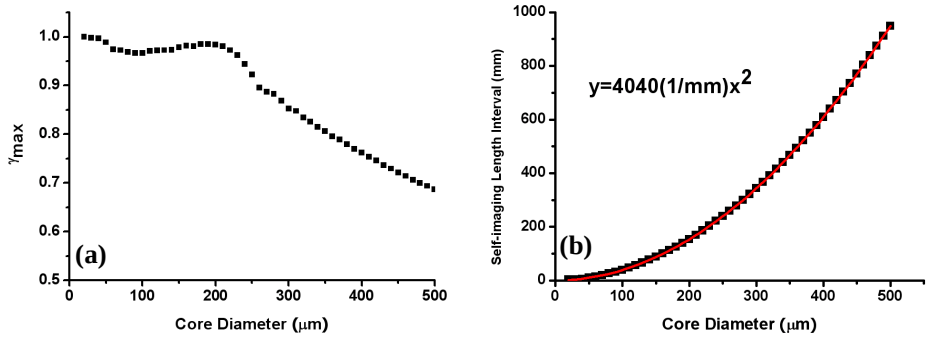

Fig. 5. (a). The maximum self-imaging quality factor γ_{max} and (b) the self-imaging length interval within one meter MM fiber segment of different core diameters.

3.3 Required accuracy of the multimode fiber length

Based on the analyses above, the essence of MMI fiber lasers and amplifiers is to accurately control the length of the MM fiber segment, i.e., the length should correspond exactly to the self-imaging positions shown in Fig. 3 and Fig. 5(b). After magnifying the self-imaging peaks at 10.3 and 43.28 mm in Figs. 3(a) and 3(b) and re-plotting them in Figs. 6(a) and 6(b), respectively, we can conclude that, a tolerance of < 100 μm on length is required for a self-imaging quality $\gamma > 0.9$. We should note that, cleaving a fiber of tens of centimeters long with an accuracy of < 10 μm can be achievable with commercial laboratory equipments. Moreover, thanks to the heat generation inside the active MM fiber when it is pumped, the MM fiber length can be further controlled with an accuracy of 1 μm through the thermal expansion. Therefore a self-imaging quality with the peak value can be obtained with existing technologies.

#100268 - $15.00 USD Received 18 Aug 2008; revised 18 Sep 2008; accepted 28 Sep 2008; published 2 Oct 2008

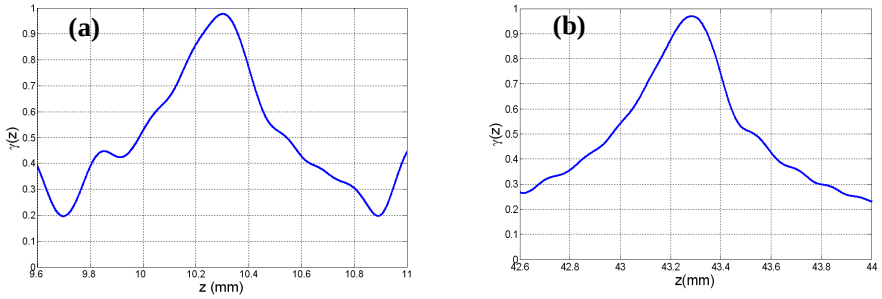

Fig. 6. Two peaks of z = 10.3 and 43.28 mm in Fig. 3(a) and (b) are magnified in (a) and (b), respectively.

It is noted that a tolerance less than 100 μm on the length is strictly required for the single-frequency operation of a MMI fiber laser or fiber amplifier. For the case of non-single-frequency operation, the required tolerance can be relaxed significantly. As shown in [16], although the active MM fiber length was not accurately controlled and changed with the pump power because of the thermal expansion, the efficiency of the MMI fiber laser did not reduce because self-imaging in the active MM fiber segment was maintained through the self-organized wavelength shift, i.e., the emission peak shifts towards shorter wavelength as the length of the MM fiber segment increased at higher pump level.

3.4 Improved self-imaging using single-mode fiber with large mode-field diameter

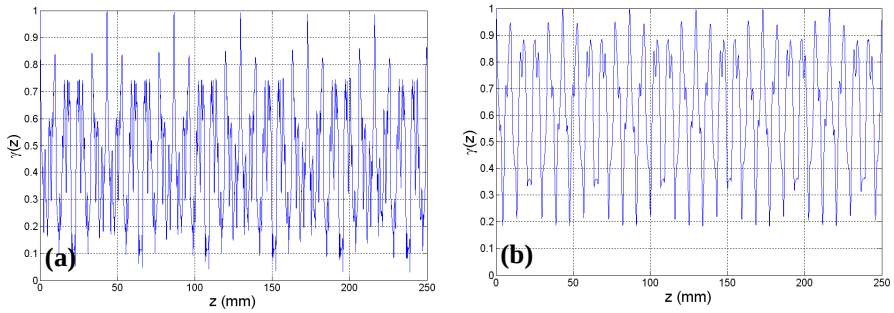

Fig. 7. Self-imaging quality factor γ along a MM fiber segment with a core diameter of 105 μm when the input SM fiber has a MFD of 23 μm and 40 μm, respectively. (a) MFD = 23 μm; (b) MFD = 40 μm.

As discussed above, the self-imaging quality reduces with the core diameter of the MM fiber segment. However, it is found that increasing the mode-field diameter (MFD) of the input SM field can improve the self-imaging quality of large-core MM fibers. Our calculations indicate that fewer guided modes are excited inside the MM fiber segment as the MFD of the input SM fiber increases and, as a consequence, the self-imaging quality is increased correspondingly. When the MFD of the input SM fiber is 23 μm and 40 μm, the number of the excited modes in the 105 μm MM fiber segment reduces to 7 and 5, respectively, as compared to 14 excited modes for a SMF-28. In the two cases, the self-imaging quality factor γ along the 105 μm MM fiber are plotted in Figs. 7(a) and 7(b), respectively. Comparing to the self-imaging quality in Fig. 3(b), not only is the self-imaging quality improved, but also the tolerance on the fiber

#100268 - $15.00 USD Received 18 Aug 2008; revised 18 Sep 2008; accepted 28 Sep 2008; published 2 Oct 2008

length is relaxed. The relaxed tolerance regarding the length of the MM segment can also be attributed to fewer excited modes in the MM fiber segment. When the MFD of the input SM fiber is 40 μm, a tolerance of 1 mm is enough to obtain a self-imaging quality higher than 0.9.

4. Experimental investigation of self-imaging in large-core multimode optical fibers

To confirm the feasibility of MMI fiber lasers and amplifiers via large-core MM fibers, the self-imaging properties of MM fibers with core diameters of 50 μm and 105 μm and a NA of 0.22 are experimentally investigated. Some key parameters to describe the self-imaging properties are also defined and evaluated quantitatively in this section.

4.1 Self-imaging behavior in wavelength representation

Instead of using many MM fiber segments with accurately-controlled lengths, the self-imaging properties of MM fibers were experimentally investigated using a few MM fiber segments with fixed lengths and a wavelength-tunable signal source or a white-light source. At the output end of the MM fiber segment of the MMI structure depicted in Fig.1, the self-imaging occurs at certain wavelengths which satisfies the following condition derived from the Eq. (4),

$$\Delta n_{eff,n} L = m_n \lambda , \qquad (m_n \text{ integer}, n = 2, 3, \ldots, N) \tag{5}$$

where L is the MM fiber length, λ is the signal wavelength, and $\Delta n_{eff,n} = (\beta_n - \beta_1)\lambda / 2\pi$.

Derived from Eq. (5) by taking the differential of λ and L, respectively, two important parameters that describe the self-imaging properties in spectrum domain, the wavelength interval of self-imaging $\Delta\lambda_{im}$ and the wavelength shift relative to the change of the MM fiber length $d\lambda/dL$, can be given by individual formula for each excited modes as follows,

$$\Delta\lambda_{im,n} = \frac{1}{\frac{L}{\lambda}\left|\frac{d\Delta n_{eff,n}}{d\lambda} - \frac{\Delta n_{eff,n}}{\lambda}\right|} \tag{6}$$

$$\frac{d\lambda_n}{dL} = \frac{1}{L\left(\frac{1}{\lambda} - \frac{1}{\Delta n_{eff,n}}\frac{d\Delta n_{eff,n}}{d\lambda}\right)} \tag{7}$$

Although $\Delta\lambda_{im}$ and $d\lambda/dL$ are the collective behavior of each individual excited mode expressed by Eq. (6) and Eq. (7) and can be only evaluated from numerical approach, a conclusion can be drawn from the above equations that both $\Delta\lambda_{im}$ and $d\lambda/dL$ are inversed to the length of the MM fiber segment. In other words, the wavelength interval of self-imaging decreases with the MM fiber length and the shift of the self-imaging wavelength due to the variation of the fiber length is small when the MM fiber segment is long. In laboratory, the length control of the MM fiber segment is flexible and oriented if $\Delta\lambda_{im}$ and $d\lambda/dL$ are known. However, since both parameters defined by Eq. (6) and Eq. (7) depend on the total length of the MM fiber segment, it is necessary to define two new parameters independent of the fiber length, $\Delta\lambda_{im}L$ and $d\lambda/(dL/L)$. Parameters of individual mode, $\Delta\lambda_{im,n}L$ and $d\lambda_n/(dL/L)$, of the 50 μm and 105 μm fiber are plotted in Fig. 8. Based on the behavior of the individual parameters, the following conclusions can be drawn for $\Delta\lambda_{im}L$ and $d\lambda/(dL/L)$: (1) wavelength dependence of $\Delta\lambda_{im}L$ is very small; (2) $d\lambda/(dL/L)$ is negative, indicating that the self-imaging wavelength shifts towards shorter wavelength as the fiber length increases; (3) $\Delta\lambda_{im}L$ of the

#100268 - $15.00 USD Received 18 Aug 2008; revised 18 Sep 2008; accepted 28 Sep 2008; published 2 Oct 2008

50 μm fiber is smaller than that of the 105 μm fiber; and (4) |dλ/(dL/L)| of the 50 μm fiber is larger than that of the 105 μm fiber.

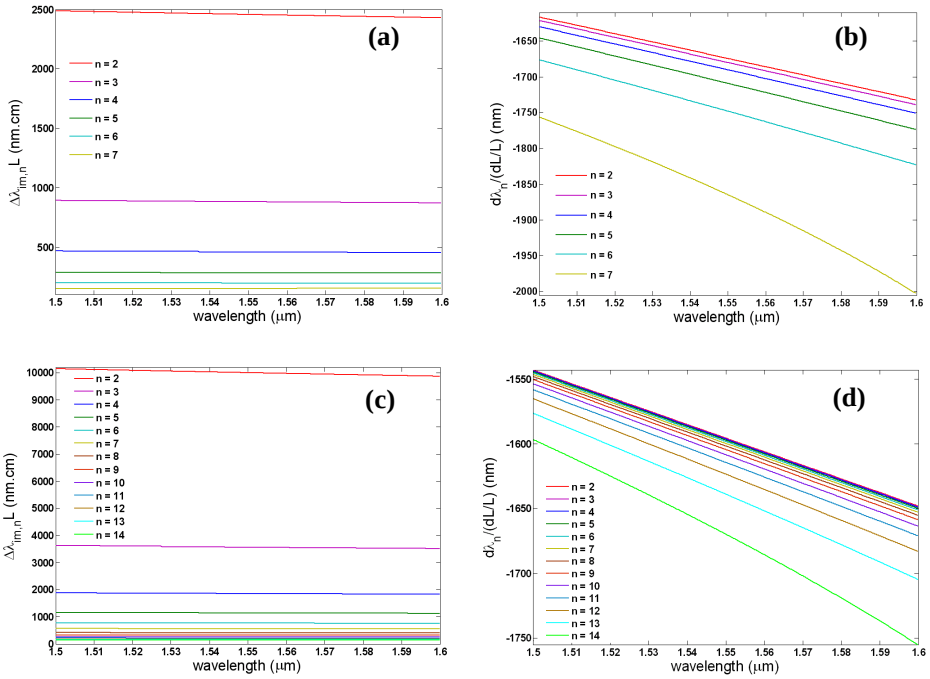

Fig. 8. Individual parameters, $\Delta\lambda_{im,n}L$ and $d\lambda_n/(dL/L)$, of the 50 μm and 105 μm fiber are plotted in a wavelength range of 1.5-1.6 μm, respectively. (a) $\Delta\lambda_{im,n}L$ of the 50 μm fiber; (b) $d\lambda_n/(dL/L)$ of the 50 μm fiber; (c) $\Delta\lambda_{im,n}L$ of the 105 μm fiber; (d) $d\lambda_n/(dL/L)$ of the 105 μm fiber.

To experimentally investigate the behavior of self-imaging in the wavelength domain, the transmission spectrum of a MMI structure, as illustrated in Fig. 9, is measured with the length of the MM fiber segment varied. A fiber-coupled white light source was employed as the input source and SMF-28 was used for the SM fiber segments.

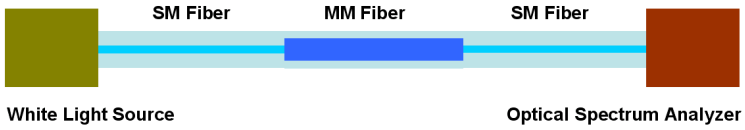

Fig. 9. Experimental setup for the transmission spectrum measurement of an MMI structure.

The transmission spectra of the MMI structure incorporating 50 μm and 105 μm MM fibers were measured for two different lengths of 20 cm and 100 cm of the MM fiber segment and are shown in Fig. 10. Clearly, the experimental results agree well with the predictions based on Eqs. (6) and (7) that are discussed above, i.e., the wavelength interval of self-

#100268 - $15.00 USD Received 18 Aug 2008; revised 18 Sep 2008; accepted 28 Sep 2008; published 2 Oct 2008

imaging $\Delta\lambda_{im}$ in the L=100 cm long MM fiber is smaller than that in the L=20 cm long MM fiber and the wavelength interval of self-imaging in the 105 μm fiber is larger than that in the 50 μm fiber because, as mentioned above, $\Delta\lambda_{im}L$ of the 105 μm fiber is larger than that of the 50 μm fiber.

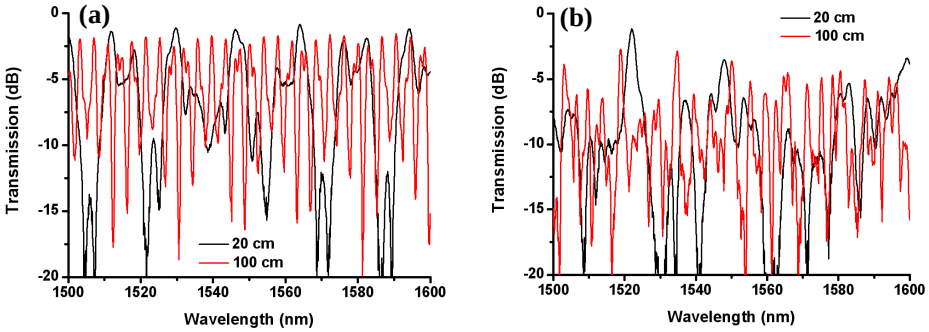

Fig. 10. Transmission spectra of MMI structures with fiber lengths of 20 cm and 100 cm and with fiber core diameters of 50 μm and 105 μm, respectively. (a) Spectra of the 50 μm fiber; (b) Spectra of the 105 μm fiber.

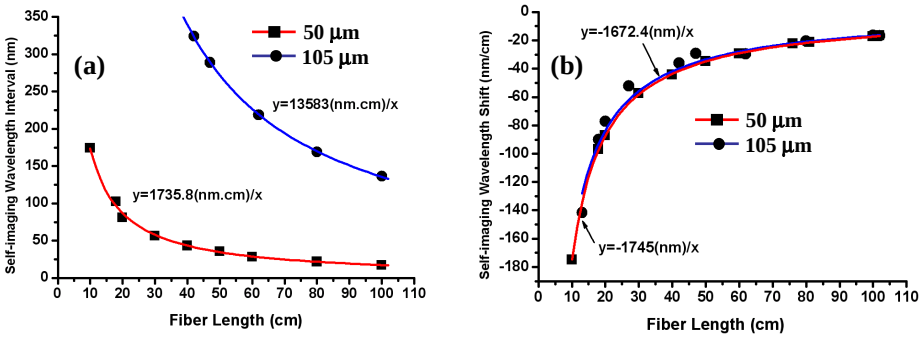

Fig. 11. The self-imaging wavelength interval and the self-imaging wavelength shift for 1 cm change of the fiber length of the MMI structure with different MM fiber lengths. (a) The wavelength interval of the self-imaging; (b) The self-imaging wavelength shift for 1 cm change of the fiber length.

To obtain the values of $\Delta\lambda_{im}L$ and $d\lambda/(dL/L)$ of self-imaging in the 50 and 105 μm MM fiber, MM fiber segments with different lengths were cut down with length intervals of 0.5 - 1 cm and the transmission spectra of the corresponding MMI structures were measured. The wavelength interval $\Delta\lambda_{im}$ and the wavelength shift $d\lambda/dL$ for 1 cm change of the MM fiber length can be obtained from the measured transmission spectra. The experimental results of $\Delta\lambda_{im}$ and $d\lambda/dL$ for the 50 and 105 μm fiber are plotted in Figs. 11(a) and 11(b), respectively. Here again, self-imaging wavelengths are defined as periodical transmission peaks with maxima clearly larger than those of their neighboring peaks. The parameters $\Delta\lambda_{im}L$ and $d\lambda/(dL/L)$ can be obtained through fitting the experimental data with a reciprocal function. As shown in Fig. 11, $\Delta\lambda_{im}L$ of the 50 and 105 μm fiber are 1735.8 and 13583 nm·cm, respectively and $d\lambda/(dL/L)$ of the 50 and 105 μm fiber are -1745 and -1672.4 nm, respectively.

#100268 - $15.00 USD Received 18 Aug 2008; revised 18 Sep 2008; accepted 28 Sep 2008; published 2 Oct 2008

It should be noted that, since $d\lambda/(dL/L)$ slightly depends on the wavelength, as shown in Figs. 8(b) and (c), the values we obtained are the average of $d\lambda/(dL/L)$ in the wavelength range of 1.5-1.6 μm.

It is noted that, in the first demonstration of a MMI fiber laser [16], a piece of 10 cm long active MM phosphate fiber with a core diameter of 25 μm was selected under a consideration of alleviating the mode conversion inside the MM fiber segment. Our experimental results indicated that, when the length and the core diameter of the MM fiber segment are small, the effect of random mode conversion induced by internal perturbations, such as core inhomogeneities, geometrical imperfection, and microbending, can be neglected. As the core diameter and the length of the MM fiber segment increase, the mode conversion becomes significant. To investigate the mode conversion in large-core passive fibers, the transmission at the self-imaging wavelength can be obtained from the transmission spectrum from the cutback experiment described above and is plotted in Fig. 12. Because the background loss of the passive MM fiber used in the experiments is very small (< 0.01dB/m in the wavelength range of 1.5-1.6 μm), the loss caused by the random mode conversion in the MM fiber can be estimated from the slope of a linear fitting of the data shown in Fig. 12. The loss due to the mode conversion in the 50 μm fiber is about 1.28 dB/m and about 1.67 dB/m in the 105 μm fiber.

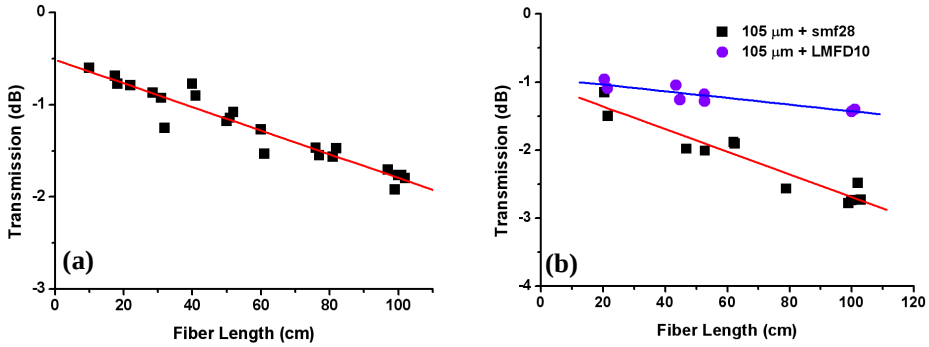

Fig. 12. Transmission at the self-imaging wavelength for MMI structures with different MMI fiber lengths. (a) Transmission at the self-imaging wavelength for MMI structures consist of a 50 μm MM fiber and a SMF-28; (b) Transmission at the self-imaging wavelength for MMI structures consist of a 105 μm MM fiber and a SMF-28 (square) or a LMFD-10 (circle), respectively.

To evaluate the improvement of self-imaging via a SMF with a large MFD as discussed in section 3.4, a passive SM fiber (LMFD-10) with a core diameter of 10 μm and a NA of 0.07 (i.e., about 23 μm of the MFD) was used to replace the SMF-28 in Fig. 9. The result of a cutback experiment for the LMFD-10 SM fiber and the 105 μm MM fiber is shown in Fig. 12(b). Obviously, the use of LMFD-10 not only improves the transmission at the self-imaging wavelength significantly (i.e., improvement of the self-imaging quality), but reduces the loss of the mode conversion as well.

4.2 Direct observation of self-imaging in multimode optical fibers

To directly observe self-imaging in the MM fiber, the field intensity distribution at the facet of the MM fiber segment of an experiment setup, as depicted in Fig. 13, was measured. A fiber-coupled single-frequency semiconductor laser with a wavelength-tunable range of 1456-1584 nm was employed as the input source. The intensity distributions at the MM fiber output facet

#100268 - $15.00 USD Received 18 Aug 2008; revised 18 Sep 2008; accepted 28 Sep 2008; published 2 Oct 2008

and of the corresponding far-field pattern were recorded by an infrared CCD camera. Self-imaging in the MM fiber was observed by tuning the wavelength of the input signal. After recording the intensity distribution, the transmission spectrum of the corresponding MMI structure was also measured by splicing the whole fiber segment to a SM fiber segment and using the experimental setup shown in Fig. 9.

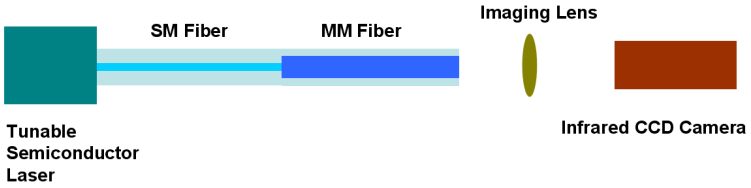

Fig. 13. Experimental setup for direct observation of self-imaging in a MM fiber.

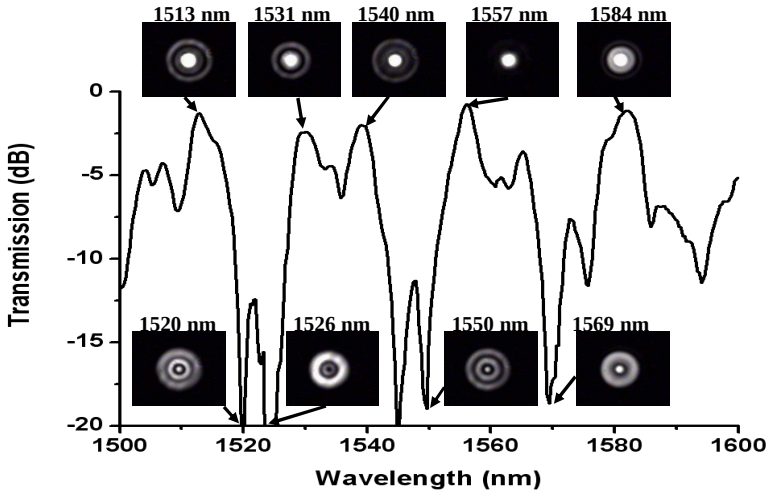

Fig. 14. The intensity distribution of the facet of the 50 μm MM fiber segment of a MMI structure when a tunable single-frequency signal is launched and the transmission spectrum of the corresponding MMI structure.

When a 15.0 cm long 50 μm MM fiber was used, the transmission spectrum and some typical intensity profiles at the MM fiber facet are shown in Fig. 14. Obviously, different intensity distributions were observed due to the complicated interference among the excited modes in the 50 μm MM fiber. When the signal wavelength λ equals 1513, 1531, 1540, 1557, or 1584 nm, the field has a very bright spot at the center of MM fiber and the corresponding transmission is large. Especially, at 1557 nm, the transmission is maximum (- 0.75 dB) in the wavelength range and the intensity distribution at the MM fiber facet resembles the input field of the SM fiber. Therefore, 1557 nm is regarded as the self-imaging wavelength, and the low-intensity image of the MM fiber facet, the corresponding three-dimensional plot, and the far-field image are shown in Fig. 15. All results indicate that high-quality self-imaging can be obtained in the 50 μm MM fiber.

#100268 - $15.00 USD Received 18 Aug 2008; revised 18 Sep 2008; accepted 28 Sep 2008; published 2 Oct 2008

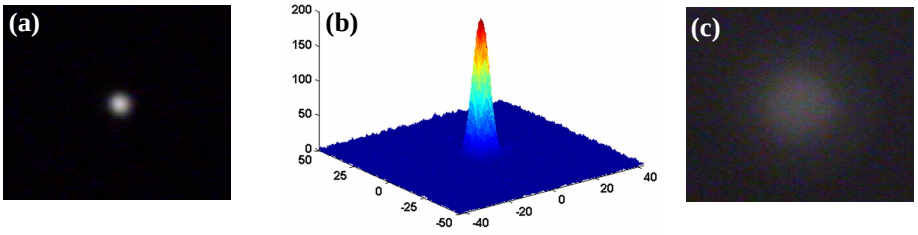

Fig. 15. The facet image, its three-dimensional plot, and the far-field image of the 50μm MM fiber segment of a MMI structure when a signal of 1557 nm is input. (a) MM fiber facet image; (b) Three-dimensional plot of (a); (c) Far-field image.

When a 12.9 cm long 105 μm fiber was used in the same experiment, the self-imaging wavelength was found to be 1575 nm. The image of the intensity distribution at the MM fiber facet, the corresponding three-dimensional plot, and the far-field image are shown in Fig. 16. Comparing the facet and the far-field intensity distributions in Figs. 16 and 17, it can be concluded that self-imaging in the 105 μm fiber is not as good as that in the 50 μm fiber.

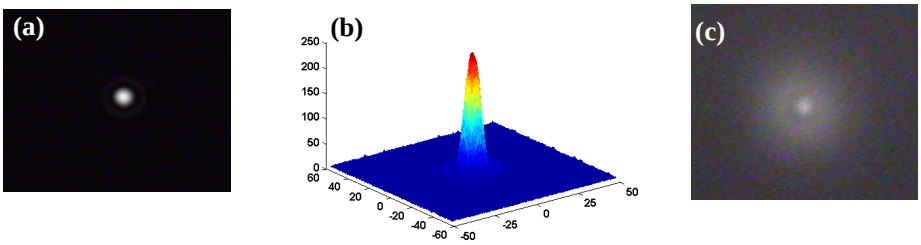

Fig. 16. The facet image, its three-dimensional plot, and the far-field image of a 105 μm MM fiber segment of a MMI structure when a signal of 1575 nm is input. (a) MM fiber facet image; (b) Three-dimensional plot of (a); (c) Far-field image.

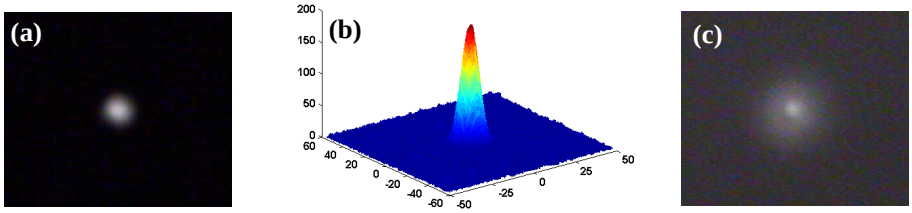

Fig. 17. The facet image, its three-dimensional plot, and the far-field image of a 105 μm MM fiber segment when a signal at the self-imaging wavelength is input and a LMFD-10 fiber is used. (a) MM fiber facet image; (b) Three-dimensional plot of (a); (c) Far-field image.

In order to confirm the improvement of self-imaging using a SM fiber with a large MFD, a LMFD-10 fiber was used as the input fiber in an experiment for the 105μm fiber. When the wavelength of the input signal is 1535 nm, the image of the intensity profile at the MM fiber facet, the corresponding three-dimensional plot, and the far-field image are shown in Fig. 17.

#100268 - $15.00 USD Received 18 Aug 2008; revised 18 Sep 2008; accepted 28 Sep 2008; published 2 Oct 2008

It can be observed that the self-imaging quality has been improved. On the other hand, self-imaging in this case is still not as good as that in the 50 μm fiber, since the far-field intensity distribution in Fig. 15 resembles the far-field of the HE_{11} mode of the SMF better.

5. Discussion

Although, in general, perfect self-imaging of the input field from a SMF-28 SM fiber cannot be obtained in large-core MM fibers, our calculations show that a reproduction of the input SM field with a self-imaging quality factor of 0.9 or larger is achievable when the core diameter of the MM fiber is smaller than 250 μm. It implies that a MMI-based large-core fiber laser or amplifier with trip-loss smaller than 1 dB can be constructed. Although additional loss caused by random mode conversion becomes significant as the fiber length is increased, our experiments in section 4.1 indicate that, in a 1-m long MMI fiber cavity, a trip-loss < 2 dB can be obtained in the 50 μm fiber and < 3 dB can be obtained in the 105 μm fiber, respectively. It should be pointed out that the MM fiber segment must be kept straight to avoid the additional loss of mode conversion caused by macro-bending, so the fiber cavity should be always shorter than 1 meter in practice. We notice that, in recent years, rod-type fiber lasers [18] can generate hundreds watts output from short-length active fibers (tens of centimeters). Therefore, high power MMI fiber lasers or amplifiers are of much practicability.

As the core diameter of the MM fiber becomes large, more modes are excited and, consequently, the cavity loss increases because of the reduced self-imaging quality and the increased mode conversion. However, the gain of a cladding-pumped fiber laser normally increases with the core diameter of the active fiber. Therefore, there is a tradeoff between the gain and the loss of mode conversion when a core diameter is selected.

Nevertheless, our calculations and experiments show that the self-imaging quality and the mode conversion in very-large-core MM fibers (> 100 μm) can be improved via SM fibers with large MFD. Technically, it is easier to fabricate a passive SM fiber with large MFD than the active counterpart. Moreover, the SM fiber segment in an MMI fiber laser or amplifier can be very short, therefore it might not be necessary to consider the bending loss that typically sets a limit for the core size of an active SM fiber. Using SM fibers with large MFD is certainly a feasible route to improve the performance of very-large-core MMI fiber lasers and amplifiers.

6. Conclusion

We have provided a quantitative characterization of self-imaging in large-core MM fibers. Our calculations and experiments confirm the feasibility of MMI fiber lasers and amplifiers using large-core active MM fibers. Although, the self-imaging quality reduces with the core diameter of the MM fiber segment, our analysis and experimental results show that it can be improved using SM fiber with larger MFD.

Acknowledgments

This work is supported by the National Sciences Foundation through Grant No. 0725479 and the Arizona Technology and Research Initiative Fund.

#100268 - $15.00 USD Received 18 Aug 2008; revised 18 Sep 2008; accepted 28 Sep 2008; published 2 Oct 2008